Effects of Dilution, Polarization Ratio, and Energy Transfer on Photoalignment of Liquid Crystals Using Coumarin-Containing Polymer Films

Chunki Kim,[†] Jason U. Wallace,[†] Shaw H. Chen,*[,†,‡] and Paul B. Merkel[§]

Department of Chemical Engineering and Laboratory for Laser Energetics, University of Rochester, 240 East River Road, Rochester, New York 14623, and Department of Chemistry, Hutchison Hall, University of Rochester, Rochester, New York 14627

Received December 17, 2007; Revised Manuscript Received February 24, 2008

ABSTRACT: Orientation of a nematic liquid crystal, E-7, was investigated using coumarin-containing polymethacrylates to elucidate the roles played by the dilution of coumarin and the polarization ratio of irradiation. Dilution of coumarin by inert moieties had adverse effects on a nematic cell's number density of disclinations and its orientational order parameter in the parallel but not the perpendicular regime. In addition, both dilution of coumarin and a decreasing polarization ratio resulted in a lower extent of coumarin dimerization at crossover, X_c. The significantly reduced X_c in a homopolymer comprising triphenylamine and coumarin was attributed to the dilution of coumarin and the diminished polarization ratio caused by competing absorption with simultaneous triplet energy transfer from triphenylamine to coumarin moieties.

Introduction

As a noncontact strategy to prevent dust, electrostatic charges, and physical damage arising from mechanical rubbing, photoalignment has been extensively explored for orienting liquid crystalline fluids, π-conjugated oligomers and polymers.[1–4] In principle, photoalignment is accomplished by axis-selective degradation, cis–trans isomerization, or dimerization induced by linearly polarized irradiation of photoreactive polymer films. This concept has been demonstrated with polyimides[5–13] and polymers containing azobenzene,[14–23] cinnamate,[24–31] or coumarin[32–40] moieties for electro-optics,[22,41] wide viewing angle liquid crystal displays,[32,33] and organic field-effect transistors.[13,23,31] Furthermore, hole injection in organic polarized light-emitting diodes was facilitated using photoalignment layers modified with appropriate ingredients via physical doping or copolymerization.[19,37,38] Cycles of cis ↔ trans isomerization of azobenzene moieties in a polymer film are induced by linearly polarized irradiation to ultimately deplete cis-isomers in favor of trans-isomers all oriented perpendicular to the polarization axis of irradiation.[42–44] At some point toward this ultimate orientation of trans-isomers, overlying liquid crystal molecules can be aligned in the perpendicular direction. Alternatively, polarized UV-irradiation of a polyimide film causes preferential decomposition along the polarization axis, leaving imide moieties oriented perpendicular to an increasing degree as photodegradation proceeds. As a result, overlying liquid crystal molecules are aligned in the perpendicular direction to polarization axis. Therefore, photoalignment using an azobenzene-containing polymer or polyimide gives rise to perpendicular liquid crystal orientation. Photoalignment is accomplished with cinnamate- and coumarin-containing polymers through preferential dimerization via (2 + 2) cycloaddition under polarized UV-irradiation. In the presence of simultaneous photoisomerization, cinnamate-containing polymers tend to yield a perpendicular liquid crystal orientation. In coumarin-containing polymers, however, crossover from a parallel to a perpendicular liquid crystal orientation has been widely reported at an intermediate stage of photodimerization. It is generally understood that crossover is the result of coumarin monomers competing with dimers for dictating liquid crystal orientation.[1,34,35] It is remarked in passing that of all the photoalignment materials, coumarin-containing polymers are advantageous in thermal and photochemical stability without complication from isomerization while offering a wide range of pretilt angle.[32,33]

To interpret the crossover behavior within a quantitative framework, we have constructed a kinetic model in which the extent of photodimerization, X, was characterized for monitoring the progress in liquid crystal orientation.[39] We have chosen coumarin-containing polymers for experimentation because a sufficiently high X can be reached to enable an investigation of crossover without encountering photoinduced isomerization or degradation.[3,39] At a relatively low X, coumarin dimers form preferentially along the polarization axis of irradiation, which controls liquid crystal orientation. At a relatively high X, residual coumarin monomers are left preferentially perpendicular to the polarization axis that dictates liquid crystal orientation. Three factors have been identified for determining X at crossover (i.e., X_c): relative abundance of coumarin dimers and monomers, their orientational order parameters (i.e., S_d and S_m) as functions of X, and the energetics of interaction with liquid crystal molecules.[3,39,40] In essence, photoalignment of liquid crystals is a manifestation of chemical anisotropy presented by coumarin dimers or monomers in orthogonal directions depending on the stage of photodimerization. The chemical anisotropy was appraised as optical anisotropy, such as UV–vis absorption dichroism of irradiated films, for the determination of S_d and S_m, which is one of the thrusts of an earlier publication[40] generally applicable to the interpretation of liquid crystal orientation. The present work was motivated to discover new features of photoalignment of liquid crystals by elucidating (i) the roles played by the dilution of coumarin moieties and the polarization ratio of UV-irradiation and (ii) the effects of excited-state energy transfer and photoinduced electron transfer in a coumarin-containing polymethacrylate functionalized with triphenylamine to facilitate hole transport.

Experimental Section

Materials Synthesis. The reaction schemes as well as the synthesis and purification procedures for polymer **2** and tris(*m*-

---

* Author to whom all correspondence should be addressed.

[†] Departments of Chemical Engineering, University of Rochester.

[‡] Laboratory for Laser Energetics, University of Rochester.

[§] Department of Chemistry, University of Rochester.

10.1021/ma702809g CCC: $40.75

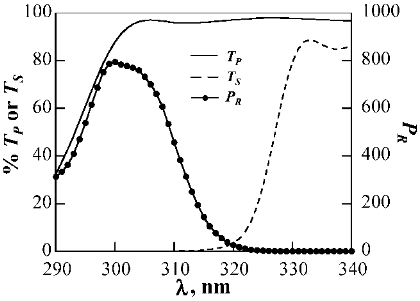

Figure 1. Polarization ratio, $P_R = T_P/T_S$, of a polarizing beam splitter with T_P and T_S denoting the maximum and minimum transmittances, respectively, of the linearly polarized incident.

anisyl)amine, **TAA**, are included in the Supporting Information and those for 7-heptyloxycoumarin, **HOC**,[39] polymers **1**,[39] **3**,[3] and **4**[3] have been reported previously. The analytical and ^{1}H NMR spectral data are presented in what follows.

Poly[3-[3-[(Methacryloyl)oxy]propyl]oxy-*N*,*N*-bis[3-[[[(coumarin-7-yl)oxy]hexyl]oxy]phenyl]benzeneamine], Polymer 2. Anal. Calcd: C, 72.75; H, 6.33; N, 1.54. Found: C, 72.47; H, 6.12; N, 1.60. ^{1}H NMR spectral data (400 MHz, $CDCl_3$): δ (ppm) 0.89–1.02 (3H, $-CH_2-C(C\mathit{H}_3)(COO-)-$), 1.31 (8H, $-CH_2CH_2C\mathit{H}_2C\mathit{H}_2CH_2CH_2-$), 1.65–2.10 (12H, $-CH_2C\mathit{H}_2CH_2-CH_2C\mathit{H}_2CH_2-$, $-C\mathit{H}_2C(CH_3)(COO-)-$, $-CH_2C\mathit{H}_2CH_2-$), 3.80–4.15 (12H, $-COOC\mathit{H}_2-$, $-C\mathit{H}_2O-Ar-$), 6.18 (2H, $-HC{=}C\mathit{H}CO-$, coumarin), 6.48–6.95 (13H, aromatics and coumarin), 7.07 (3H, aromatics), 7.30 (2H, coumarin), 7.57 (2H, $-\mathit{H}C{=}CHCO-$, coumarin).

Tris(*m*-anisyl)amine, TAA. Anal. Calcd: C, 75.20; H, 6.31; N, 4.18. Found: C, 75.23; H, 6.39; N, 4.18.^{1}H NMR spectral data (400 MHz, $CDCl_3$): δ (ppm) 3.74 (s, 9H, CH_3O-), 6.60 (d, 3H, aromatics), 6.69 (m, 6H, aromatics), 7.17 (t, 3H, aromatics).

Transition Temperatures and Polymer Molecular Weights. Thermal transition temperatures of polymers **1**−**4** were determined by differential scanning calorimetry, DSC (Perkin-Elmer, DSC-7), with a continuous N_2 purge at 20 mL/min. Samples were preheated up to 100 °C followed by cooling to −30 °C before taking the reported heating and cooling scans at 20 °C/min. The nature of phase transitions was characterized with a polarizing optical microscope (DMLM, Leica, FP90 central processor) coupled with a hot stage (FP82, Mettler Toledo). Polymer molecular weights were characterized in *N*-methylpyrrolidone containing 0.02 M lithium bromide at 60 °C using size exclusion chromatography (Model 301 TDA, Viscotek) based on a universal calibration involving polystyrene standards (Pressure Chemical Company).

Preparation and Characterization of Photoalignment Films. For the alignment of a nematic liquid crystal, films of polymers **1** and **3** were prepared by spin-casting at 4,000 rpm from 0.1 wt % chloroform solutions on optically flat fused silica substrates transparent to 200 nm (Esco Products). Films of polymers **2** and **4** were prepared by spin-casting at 3500 rpm from 0.2 wt % chloroform solutions on the same fused silica substrates. Spin-cast films were characterized with variable angle spectroscopic ellipsometry (V-Vase, J. A. Woollam Corporation) and UV–vis−NIR spectrophotometry (Lambda-900, Perkin-Elmer). Polarized irradiation was performed under argon using a 500 W Hg−Xe lamp (model 66142, Oriel) equipped with a dichroic mirror that reflects the light between 260 and 320 nm (model 66217, Oriel) and a filter (model 87031, Oriel) that cuts off wavelengths below 300 nm. In addition, linear polarization was generated using a polarizing beam splitter (HPB-308 nm, Lambda Research Optics, Inc.) with the dispersion of polarization ratio shown in Figure 1. Films of polymers **1**−**4** were irradiated at 90, 96, 120, and 142 °C, respectively, to ensure the same reduced temperature of 1.15 relative to their respective glass transition temperatures. The irradiation intensity was monitored by a UVX digital radiometer coupled with a UVX-31 sensor (UVP, Inc.). The extent of photodimerization was characterized by monitoring the UV–vis absorbance of coumarin monomers at 325 nm for polymers **1** and **2** and 310 nm for polymers **3** and **4**, respectively. The insolubility limit was established by comparing the UV–vis absorption spectra before and after rinsing the irradiated films with chloroform.

Photoalignment of a Nematic Liquid Crystal. For the characterization of their ability to orient a nematic liquid crystal, irradiated films of polymers **1**−**4** on fused silica substrates were used to prepare 10-μm-thick sandwiched cells. A commercially

Chart 1. Polymers and Model Compounds Used in This Study

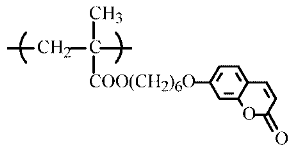

Polymer 1: T_g = 43 °C

$\overline{M}_w$ = 133,000 g/mol; $\overline{M}_w/\overline{M}_n$ = 3.9

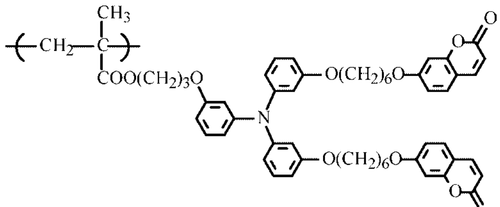

Polymer 2 : T_g = 48 °C

$\overline{M}_w$ = 242,000 g/mol; $\overline{M}_w/\overline{M}_n$ = 2.8

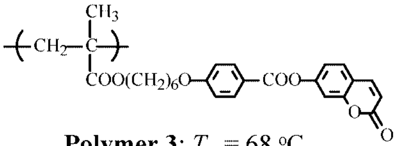

Polymer 3: T_g = 68 °C

$\overline{M}_w$ = 76,300 g/mol; $\overline{M}_w/\overline{M}_n$ = 3.3

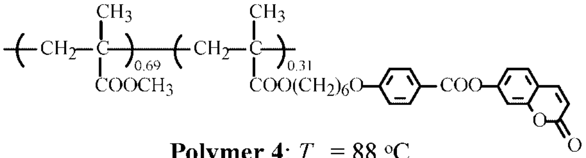

Polymer 4: T_g = 88 °C

$\overline{M}_w$ = 48,700 g/mol; $\overline{M}_w/\overline{M}_n$ = 2.1

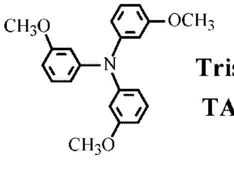

Tris(*m*-anisyl)amine, TAA

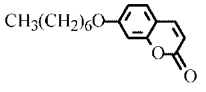

7-Heptyloxycoumarin, HOC

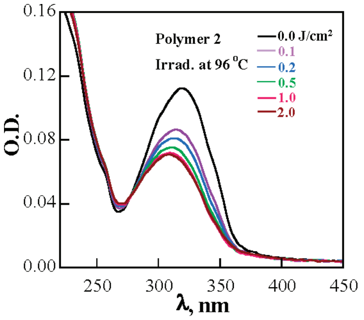

Figure 2. UV–vis absorption spectra of 15-nm-thick polymer **2** film as a function of fluence.

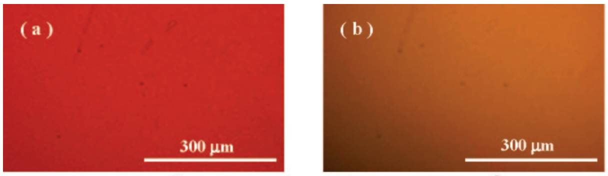

Polymer 1, 0.5 J/cm², S_{lc}= || 0.70 **Polymer 1**, 2.0 J/cm², S_{lc}= ⊥ 0.72

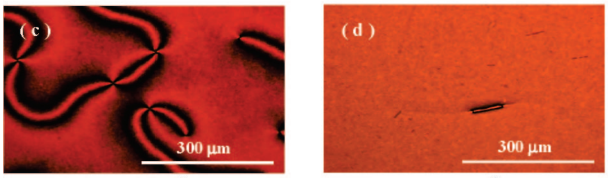

Polymer 2, 0.05 J/cm², S_{lc}= || 0.48 **Polymer 2**, 0.2 J/cm², S_{lc}= ⊥ 0.76

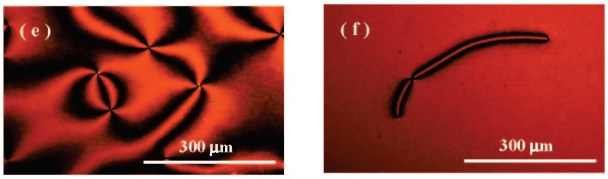

Polymer 4, 1.5 J/cm², S_{lc}= || 0.34 **Polymer 4**, 2.0 J/cm², S_{lc}= ⊥ 0.74

Figure 3. Polarizing optical microscopic images of liquid crystal cells selected from Tables 1 and 2 with their orientational order parameter values—polymer **1**, parts a and b; polymer **2**, parts c and d; polymer **4**, parts e and f—to illustrate the effects of dilution of coumarin moieties.

available nematic liquid crystal, E-7 (Merck), containing a dichroic dye, M-137 (Mitsui Toatsu Dyes, Ltd.), at 0.3 wt % was injected into the cell gap in the isotropic state (at 65 °C) to avoid flow-induced alignment. After annealing at 50 °C for 0.5 h, the cells were cooled at 10 °C/h to room temperature. The UV−vis−NIR spectrophotometer (Lambda-900, Perkin-Elmer) was equipped with a linear polarizer (HNP′B, Polaroid) for the measurement of orientational order parameter. Fresnel reflections from the air-glass interfaces were accounted for using a reference cell comprising an index-matching fluid sandwiched between two alignment-treated substrates.

Measurement of Absorption, Fluorescence, and Phosphorescence Spectra. Dilute solutions of **TAA** and **HOC** in ethyl acetate were prepared at a concentration of 10^{-4} M. The absorption spectra were gathered with UV−vis−NIR diode array (Hewlett-Packard 8453E). Fluorescence spectra were collected with a spectrofluorometer (Quanta Master C-60SE, Photon Technology International) at excitation wavelengths of 300 nm for **TAA** and 325 nm for **HOC** in a 90° orientation, respectively. Phosphorescence spectra were measured using a Fluorolog-3 spectrofluorometer (Jobin Yvon, Horiba) and were corrected for the efficiency of the monochromator and the spectral response of the photomultiplier tube. Phosphorescence was measured in ethyl acetate at 77 K by placing solutions in NMR tubes inserted into a small liquid nitrogen Dewar in a holder designed to fit the spectrofluorometer.

Table 1. Extent of Photodimerization, X, and Liquid Crystal Orientational Order Parameter, S_{lc}, as Functions of Fluence for Polymers 1 and 2

	polymer **1**[a]		polymer **2**[b]	
fluence, J/cm²	X[c]	S_{lc}[d]	X[c]	S_{lc}[d]
0.05			0.23	|| 0.48
0.1	0.37	|| 0.71	0.34	⊥0.52
0.2	0.40		0.42	⊥0.76
0.5	0.49	|| 0.70	0.51	⊥0.75
1.0	0.60	|| 0.72	0.55	⊥0.74
2.0	0.67	⊥0.72		

[a] Irradiation of 10-nm-thick films at 90 °C, and insolubility in chloroform achieved at 0.05 J/cm²; all data taken from ref 39. [b] Irradiation of 15-nm-thick films at 96 °C, and insolubility in chloroform achieved at 1.0 J/cm²; photoalignment layers below insolubility limit shown to be intact by UV−vis spectrophotometry after exposure to E-7 in liquid crystal cells. [c] X determined at 325 nm with an uncertainty of ±0.02. [d] 10-µm-thick nematic cells of E-7 doped with M-137; symbols || and ⊥ in front of S_{lc} represent a nematic director parallel and perpendicular to the polarization axis of UV-irradiation, respectively; S_{lc} determined at 643 nm with an uncertainty of ±0.02 on average.

Laser Flash Photolysis Measurements. A laser photolysis system described elsewhere[45]was used to probe radical cation formation from **TAA** and for pulsed photolysis of solutions of **TAA** and **HOC**. A XeCl excimer laser (Lambda Physik Lextra 50) was used to pump a dye laser (Lambda Physik 3002) containing *p*-terphenyl, which provided 7-ns approximately 1 mJ pulses at 343 nm. Transient absorptions were monitored at 90° to the laser excitation using a pulsed xenon lamp, timing shutters, a monochromator, and a diode array detector.

Characterization of a Polarizing Beam Splitter's Polarization Ratio. The UV−vis−NIR spectrophotometer (Lambda-900, Perkin-Elmer) equipped with a linear polarizer (HNP′B, Polaroid) was used to characterize the polarization ratio of a polarizing beam splitter (HPB-308 nm, Lambda Research Optics, Inc.) used for polarized UV-irradiation in preparation of photoalignment films.

Results and Discussion

The molecular structures of all the materials used in this study are depicted in Chart 1. While polymers **1**, **3**, and **4** have been reported elsewhere,[3,39] polymer **2** was synthesized as part of this work to incorporate hole-transporting triphenylamine with coumarin in a homopolymer. Stability against degradation of polymers **1**−**4** during the preparation of photoalignment films was validated with UV–vis absorption spectra exhibiting isosbestic points, as illustrated in Figure 2 using polymer **2**, over the irradiation intensity (i.e., fluence) range to include crossover in the orientation of E-7. The nematic director of 10-µm-thick E-7 cells was tracked by a dichroic dye, M-137 with an absorption maximum at 643 nm, at a doping level of 0.3 wt % as described previously.[3,39,40] Linearly polarized absorption spectra, as illustrated on polymer **2** in the Supporting Information, were collected to evaluate the absorption dichroism at 643 nm for the calculation of the orientational order parameter, $S_{lc} = (R - 1)/(R + 2)$, where the dichroic ratio R represents the absorbance parallel divided by that perpendicular to the polarization axis of UV-irradiation.

The coumarin contents in polymers **1** and **3** are diluted by triphenylamine and methyl moieties in polymers **2** and **4**, respectively. Dilution of coumarin deteriorated the quality of nematic liquid crystal cells and their orientation order parameter, S_{lc}. Polymers **1** and **3** films were capable of producing liquid crystal cells without disclinations, as illustrated with polymer **1** in Figure 3, parts a and b. As a consequence, all the S_{lc} values reported for polymers **1** and **3** in Tables 1 and 2 are greater than or equal to 0.70, in which the prefixes || and ⊥ to the S_{lc} values indicate a parallel and a perpendicular orientation, respectively, of the nematic director to the polarization axis of irradiation. In contrast, the liquid crystal cells on polymers **2**

Table 2. Extent of Photodimerization, *X*, and Liquid Crystal Orientational Order Parameter, S_{lc}, as Functions of Fluence for Polymers 3 and 4

	polymer 3[a]		polymer 4[b]	
fluence, J/cm^2	*X*[c]	S_{lc}[d]	*X*[c]	S_{lc}[d]
0.1	0.18		0.11	
0.2	0.24	$\parallel$ 0.73	0.16	$\parallel$ 0.43
0.5	0.35	$\parallel$ 0.75	0.26	$\parallel$ 0.51
1.0	0.45	$\parallel$ 0.71	0.35	$\parallel$ 0.56
1.5			0.43	$\parallel$ 0.34
2.0	0.53		0.46	$\perp$0.74
4.0	0.57	$\parallel$ 0.73		
5.0	0.59	$\perp$0.80		

[a] Irradiation of 10-nm-thick films at 120 °C, and insolubility in chloroform achieved at 0.2 J/cm^2; all data taken from ref 3. [b] Irradiation of 18-nm-thick films at 142 °C, and insolubility in chloroform achieved at 0.5 J/cm^2; photoalignment layer below insolubility limit shown to be intact by UV−vis spectrophotometry after exposure to E-7 in liquid crystal cell. [c] *X* determined at 310 nm with an uncertainty of ±0.02. [d] 10-μm-thick nematic cells of E-7 doped with M-137; symbols $\parallel$ and $\perp$ in front of S_{lc} represent a nematic director parallel and perpendicular to the polarization axis of UV-irradiation, respectively; S_{lc} determined at 643 nm with an uncertainty of ±0.04 on average.

and **4** contained a higher number density of disclinations in the parallel regime than that on polymers **1** and **3**, as displayed in Figure 3, parts c and e. As a result, the S_{lc} values with polymers **2** and **4** are substantially less than 0.60 in the parallel regime, where coumarin dimers control liquid crystal orientation. Both the number density of disclinations (Figure 3, parts d and f, versus Figure 3b) and the S_{lc} values (see Tables 1 and 2), however, are comparable to those without dilution of coumarin moieties in the perpendicular regime, where coumarin monomers dictate liquid crystal orientation. The observed difference between the two regimes associated with polymers **2** and **4** could have arisen from the stronger molecular interaction of E-7 with coumarin monomers[34,35] and/or the better orientational order on the part of coumarin monomers compared to coumarin dimers.[39] These results suggest that perpendicular orientation should be the target of photoalignment of liquid crystals on polymer **2** and other functionalized polymers for the realization of highly oriented monodomain nematic films.

It is further noted in Table 2 that the dilution of coumarin moieties expedited the crossover from $X_c \cong 0.58$ on polymer **3** to 0.45 on polymer **4**. As dilution caused both coumarin dimers and monomers to be less ordered in the parallel and perpendicular direction, respectively, the lower X_c for polymer **4** than **3** can be understood in terms of the stronger interaction of liquid crystal molecules with coumarin monomers than dimers.[34,35] Across the irradiation fluence from 0.1 to 20.0 J/cm^2, the *X* and S_{lc} values observed on 10-nm-thick polymer **1** films were identical with those on 27-nm-thick films within experimental uncertainties,[39] as expected of photoalignment being a surface phenomenon. Therefore, the *X* and S_{lc} values reported in Tables 1 and 2 should be independent of the photoalignment film thickness varying from 10 to 18 nm to facilitate film preparation and characterization.

Table 3. Case Studies Using Polymer 3 for Evaluation of S_{lc} as a Function of the Extents of Dimerization Contributed by Polarized (X_p) and Unpolarized (X_u) Irradiation at Room Temperature for the Same Cumulative $X = 0.35$[a]

case	first irradiation	second irradiation	S_{lc}
A	$X_p = 0.27$	$X_u = 0.08$	$\parallel$ 0.73
B	$X_u = 0.07$	$X_p = 0.28$	$\parallel$ 0.73
C	$X_u = 0.28$	$X_p = 0.07$	$\perp$ 0.71
D	$X_p = 0.07$	$X_u = 0.28$	$\perp$ 0.72

[a] 10-μm-thick nematic cells of E-7 doped with M-137; symbols $\parallel$ and $\perp$ in front of S_{lc} represent a nematic director parallel and perpendicular to the polarization axis of UV-irradiation, respectively. X_p, X_u, and S_{lc} all accompanied by an experimental uncertainty of ±0.02.

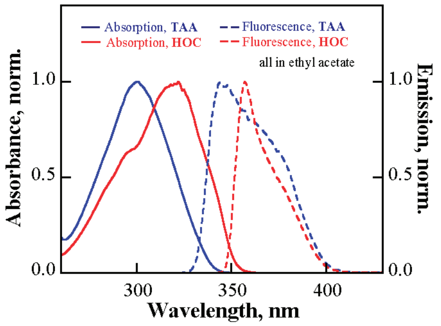

Figure 4. Normalized absorption and fluorescence spectra of **TAA** and **HOC** in ethyl acetate at 10^{-4} M measured at room temperature.

To examine the effect of polarization ratio on crossover, four cases were investigated with mixed modes of irradiation using polymer **3**. The results summarized in Table 3 reveal the critical role played by the extent of dimerization induced by polarized, X_p, relative to that by unpolarized, X_u, irradiation for the same cumulative $X = X_p + X_u = 0.35$ in all cases regardless of the order in which the two modes of irradiation were administered. As suggested by the data for cases A and B, a parallel liquid crystal orientation emerged where polarized irradiation was dominant. The reason is that coumarin dimers formed are better ordered parallel than residual monomers perpendicular to the polarization axis at the early stage of photodimerization. In contrast, a perpendicular liquid crystal orientation prevailed where unpolarized irradiation was dominant, as in cases C and D. In these two cases, both coumarin dimers and residual monomers are expected to be poorly ordered parallel and perpendicular, respectively, to the polarization axis because of the predominant extents of dimerization completed under unpolarized excitation. A possible outcome of the low orientational order on the parts of coumarin monomers and dimers could have been diminished S_{lc} values in cases C and D. The fact that E-7 molecules turned out to be well aligned with coumarin monomers is attributable to the favorable energetics of molecular interaction over coumarin dimers, as rationalized by Ichimura et al.[34] and Kelly et al.,[35] coupled with a sufficient orientatioanl order adopted by coumarin monomers. To sum up, a high polarization ratio of irradiation received by coumarin produced a parallel liquid crystal orientation, whereas a low polarization ratio generated a perpendicular orientation. In other words, X_c decreases with a decreasing polarization ratio under otherwise identical conditions.

We now proceed to photoalignment on polymer **2** incorporating both coumarin and triphenylamine moieties. As shown in Table 1, crossover from a parallel to a perpendicular orientation occurred at $X_c \cong 0.64$ and 0.29 on polymers **1** and **2**, respectively. On the basis of the foregoing comparison between polymers **3** and **4** as well as the case studies using polymer **3**, two factors can be identified as the potential origins of the substantially lower X_c on polymer **2** than **1**: dilution of coumarin by triphenylamine and the lower polarization ratio of irradiation received by coumarin for photodimerization. A lower polarization ratio received by coumarin in polymer **2** than polymer **1** is attributable to competing absorption of polarized irradiation between triphenylamine and coumarin, and simultaneous triplet energy transfer from triphenylamine to coumarin moieties. Two model compounds, previously reported **HOC**[39] and **TAA** synthesized herein, were used to evaluate these two contributing factors. The absorption spectra of **TAA** and **HOC** in ethyl acetate (see Supporting Information), an analogue for the methacrylate polymer backbone, suggest that the two moieties absorb the UV-irradiation to comparable extents. In view of the wavelength dependence of polarization ratio displayed in Figure 1, coumarin moieties absorb less in the high polarization

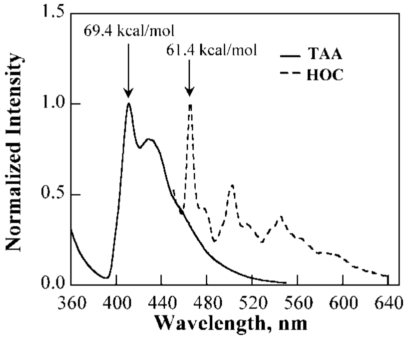

Figure 5. Phosphorescence spectra of **TAA** and **HOC** in ethyl acetate at 10^{-4} M and 77 K.

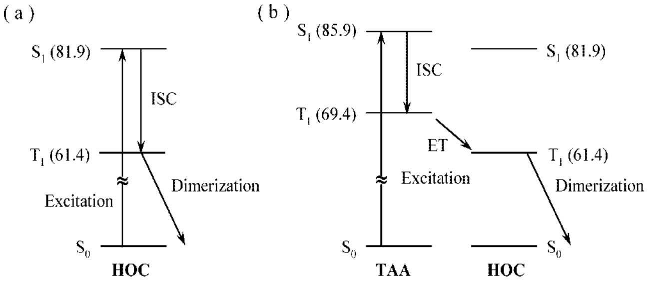

Figure 6. Schematic diagrams of molecular energy levels, S_1 and T_1, in kcal/mol, intersystem crossing (ISC), and coumarin dimerization from T_1 involving (a) **HOC** alone, and with triplet energy transfer (ET) involving (b) **TAA** and **HOC**.

ratio region than in the absence of triphenylamine moieties. In addition, absorption by triphenylamine moieties followed by triplet energy transfer to coumarin, as to be detailed below, resulted in a loss of polarization. Consequently, polarization ratio received by coumarin decreased in the presence of triphenylamine. On the basis of the correlation between liquid crystal orientation and the polarization ratio illuminated by case studies (see Table 3), X_c on polymer **2** is expected to be less than that on polymer **1**.

The role played by energy transfer from triphenylamine to coumarin moieties in polymer **2** was appraised using **HOC** and **TAA**. In the absence of triphenylamine, photoexcitation produces coumarin singlets, S_1, the lowest singlet state, with a fluorescence quantum yield on the order of 0.01.[46] Such a low quantum yield implies efficient nonradiative decays of S_1, including intersystem crossing to T_1, the lowest triplet state, which contributes predominantly to dimerization.[46] In addition, a fluorescence quantum yield less than 0.1 was reported for triphenylamine.[47] The wavelengths at which the normalized absorption and fluorescence spectra intersect, as shown in Figure 4, were employed to determine the S_1 energy levels[48] for **TAA** and **HOC** at 85.9 and 81.9 kcal/mol, respectively.

The phosphorescence spectra were gathered for **TAA** and **HOC** at 10^{-4} M in ethyl acetate at 77 K. The normalized spectra shown in Figure 5 exhibit relatively sharp highest energy 0–0 vibronic bands assigned as the T_1 states.[49–51] The phosphorescence from **HOC** was weak relative to its fluorescence, suggesting a low quantum yield for intersystem crossing. Butyl iodide was added at 10 wt % to the **HOC** solution to enhance the 0–0 vibronic transition[52] and confirm the identity of the emitting state. Triplet energies of 69.4 and 61.4 kcal/mol were thereby obtained for **TAA** and **HOC**, respectively. The results for the S_1 and T_1 energies for the two model compounds are summarized in the diagrams presented in Figure 6.

Since electron-rich **TAA** and triphenylamine should be easily oxidized, it is conceivable that photoinduced electron transfer from triphenylamine to coumarin moieties could also play a role in the dimerization process in polymer **2** films. Laser pulse excitation at 343 nm of the electron acceptor *N*-methylquinolinium tetrafluoroborate (10^{-3} M) in an acetonitrile solution containing **TAA** (2×10^{-4} M) and 0.5 M toluene as a codonor resulted in the formation of **TAA** radical cation ($\lambda_{max} = 580$ nm) via efficient electron transfer from toluene to the sensitizer followed by electron transfer from **TAA** to toluene. However, laser photolysis of an acetonitrile solution of **HOC** (10^{-4} M) and **TAA** (10^{-3} M) resulted in only triplet species without **TAA** radical cations. This suggests that electron transfer from triphenylamine to coumarin moieties plays an insignificant role in the photodimerization of coumarin in polymer **2**. Both the triphenylamine and coumarin moieties undergo S_1-to-T_1 intersystem crossing but with very different quantum yields, 0.88 for triphenylamine.[53]] versus generally less than 0.05 for coumarin.[54] The substantially higher triplet energy of **TAA** than **HOC** implies that the triplet energy transfer from triphenylamine to coumarin moieties in polymer **2** films is quite exothermic and hence very efficient. In this process, the polarization of irradiation is lost.[55] Depolarization of photoexcitation is expected on the basis of the triplet–triplet energy transfer within the Dexter formalism involving no orientational factors,[56] where coumarin moieties are randomly oriented with the photosensitizing triphenylamine moieties. The two empirical observations of polarization-preserved triplet–triplet energy transfer appear to have arisen from the alignment of cinnamate moieties with photosensitizers, as evidenced by the reported exciplex formation[57,58] and the enhanced polarization retention with a photosensitizer's rod-like molecular shape.[59] A short-range alignment of cinnamate moieties with photosensitizers permits the polarization-selective absorption by the latter to be transferred to the former as an exception to the rule.[56]

Thus, triplet energy transfer from triphenylamine to coumarin moieties substantially decreased the polarization ratio of irradiation received by coumarin for photodimerization. In a nutshell, functionalization of coumarin-containing polymer with triphenylamine for photoalignment of E-7 reduced considerably the X_c value because of dilution as well as the diminished polarization ratio received by coumarin due to competing absorption and triplet energy transfer. Nevertheless, the relative contributions of these three factors to the observed photoalignment behavior can not be quantified at this time. Work is in progress to evaluate the efficiency and lifetime of organic polarized light-emitting diodes using hole-conducting photoalignment polymers comprising both the hole-transporting and coumarin moieties, and the results will be reported in due course.

Summary

Four coumarin-containing polymethacrylates were employed to furnish new insight into the effects of dilution of coumarin, polarization ratio of UV-irradiation, excited-state energy transfer, and photoinduced electron transfer on the photoalignment of E-7. The extent of coumarin dimerization at crossover, X_c, was found to decrease with dilution of coumarin by photophysically inert moieties. Moreover, dilution of coumarin was responsible for a higher number density of disclinations in liquid crystal cells accompanied by lower S_{lc} values in the parallel regime. These adverse effects, however, were absent in the perpendicular regime beyond crossover. Case studies using a polymer consisting exclusively of coumarin under mixed modes of polarized and unpolarized irradiation revealed a decreasing X_c with a diminishing polarization ratio. Tris(*m*-anisyl)amine and 7-heptyloxycoumarin were used to probe competing absorption, triplet energy transfer, and photoinduced electron transfer from triphenylamine to coumarin moieties in a homopolymer comprising both coumarin and triphenylamine moieties. Competing absorption of polarized UV-irradiation between coumarin and triphenylamine reduced the polarization ratio received by coumarin moieties. Furthermore, the triplet energies associated with these two model compounds suggest efficient triplet energy transfer, resulting in a loss of polarization ratio received by coumarin moieties. Nevertheless, photoinduced electron transfer from triphenylamine to coumarin played an insignificant role in coumarin dimerization on the basis of laser photolysis. Therefore, dilution of coumarin and competing absorption of polarized irradiation with simultaneous triplet energy transfer from triphenylamine to coumarin moieties all contributed to the much lower X_c for polymer **2** than **1**, 0.29 in contrast to 0.64.

Acknowledgment. The authors thank Stephen D. Jacobs and Kenneth L. Marshall of the Laboratory for Laser Energetics, LLE, at University of Rochester for helpful discussions and technical advice. They are grateful for the financial support provided by the Eastman Kodak Company, the New York State Center for Electronic Imaging Systems, and the National Science Foundation under Grant CTS-0204827. J.U.W. acknowledges the support of a Horton Graduate Fellowship administered by the LLE. Additional funding was provided by the Department of Energy Office of Inertial Confinement Fusion under Cooperative Agreement No. DE-FC52-08NA28302 with LLE and the New York State Energy Research and Development Authority. The support of DOE does not constitute an endorsement by DOE of the views expressed in this article.

Supporting Information Available: Reaction schemes and text giving procedures for the synthesis and purification with analytical and PMR spectral data for polymer **2** and **TAA**, and figures showing the the UV–vis absorption spectra of the dilute solutions of **TAA** and **HOC** in ethyl acetate, and representative polarized UV–vis absorption spectra for the calculation of S_{lc} on photoalignment films. This material is available free of charge via the Internet at http://pubs.acs.org.

References and Notes

(1) O'Neill, M.; Kelly, S. M. *J. Phys. D: Appl. Phys* **2000**, *33*, R67–R84.
(2) Sakamoto, K.; Usami, K.; Uehara, Y.; Ushioda, S. *Appl. Phys. Lett.* **2005**, *87*, 000. 211910/1–211910/3.
(3) Trajkovska, A.; Kim, C.; Marshall, K. L.; Mourey, T. H.; Chen, S. H. *Macromolecules* **2006**, *39*, 6983–6989.
(4) Lee, J.; Lee, J.-I.; Sung, S.-J.; Chu, H. Y.; Park, J.-K.; Shim, H.-K. *Macromol. Chem. Phys.* **2004**, *205*, 2245–2251.
(5) Hasegawa, M.; Taira, Y. *J. Photopolym. Sci. Technol.* **1995**, *8*, 241–248.
(6) Lu, J.; Deshpande, S. V.; Gulari, E.; Kanicki, J.; Warren, W. L. *J. Appl. Phys.* **1996**, *80*, 5028–5034.
(7) Kim, J.-H.; Kumar, S.; Lee, S.-D. *Phys. Rev. E* **1998**, *57*, 5644–5650.
(8) Nishikawa, M.; Kosa, T.; West, J. L. *Jpn. J. Appl. Phys.* **1999**, *38*, L334–L337.
(9) Akiyama, H.; Iimura, Y. *Jpn. J. Appl. Phys.* **2000**, *41*, L521–L523.
(10) Newsome, C. J.; O'Neill, M. *J. Appl. Phys.* **2002**, *92*, 1752–1756.
(11) Xu, C.; Shiono, T.; Ikeda, T.; Wang, Y.; Takeuchi, Y. *J. Mater. Chem.* **2003**, *13*, 669–671.
(12) Zhong, Z.-X.; Li, X.; Lee, S. H.; Lee, M.-H. *Appl. Phys. Lett.* **2004**, *85*, 2520–2522.
(13) Chou, W.-Y.; Cheng, H.-L. *Adv. Funct. Mater.* **2004**, *14*, 811–815.
(14) Gibbons, W. M.; Shannon, P. J.; Sun, S.-T.; Swetlin, B. J. *Nature (London)* **1991**, *351*, 49–50.
(15) Shannon, P. J.; Gibbons, W. M.; Sun, S.-T. *Nature (London)* **1994**, *368*, 532–533.
(16) Ichimura, K.; Suzuki, Y.; Seki, T.; Hosoki, A.; Aoki, K. *Langmuir* **1988**, *4*, 1214–1216.
(17) Ichimura, K *Chem. Rev.* **2000**, *100*, 1847–1874.
(18) Chung, D. H.; Fukuda, T.; Takanishi, Y.; Ishikawa, K.; Matsuda, H.; Takezoe, H.; Osipov, M. A. *J. Appl. Phys.* **2002**, *92*, 1841–1844.
(19) Sainova, D.; Zen, A.; Nothofer, H.-G.; Asawapirom, U.; Scherf, U.; Hagen, R.; Bieringer, T.; Kostromine, S.; Neher, D. *Adv. Funct. Mater.* **2002**, *12*, 49–57.
(20) Furumi, S.; Ichimura, K. *Adv. Funct. Mater.* **2004**, *14*, 247–254.
(21) Kwok, H. S.; Chigrinov, V. G.; Takada, H.; Takatsu, H. *IEEE/OSA J. Display Technol.* **2005**, *1*, 41–50.
(22) Choi, H.; Wu, J. W.; Chang, H. J.; Park, B *Appl. Phys. Lett.* **2006**, *88*, 021905/1–021905/3.
(23) Fujiwara, T.; Locklin, J.; Bao, Z. *Appl. Phys. Lett.* **2007**, *90*, 232108/1–232108/3.
(24) Schadt, M.; Schmitt, K.; Kozinkov, V.; Chirgrinov, V. *Jpn. J. Appl. Phys.* **1992**, *31*, 2155–2164.
(25) Schadt, M.; Seiberle, H.; Schuster, A.; Kelly, S. M. *Jpn. J. Appl. Phys.* **1995**, *34*, L764–L767.
(26) Ichimura, K.; Akita, Y.; Akiyama, H.; Kudo, K.; Hayashi, Y. *Macromolecules* **1997**, *30*, 903–911.
(27) Li, X. T.; Kawakami, A.; Akiyama, H.; Kobayashi, S.; Iimura, Y. *Jpn. J. Appl. Phys.* **1998**, *37*, L743–L745.
(28) Obi, M.; Morino, S.; Ichimura, K. *Jpn. J. Appl. Phys.* **1999**, *38*, L145–L147.
(29) Shenoy, D.; Beresnev, L.; Holt, D.; Shashidhar, R. *Appl. Phys. Lett.* **2002**, *80*, 1538–1540.
(30) Kawatsuki, N.; Goto, K.; Kawakami, T.; Yamamoto, T. *Macromolecules* **2002**, *35*, 706–713.
(31) Jin, S.-H.; Seo, H.-U.; Nam, D.-H.; Shin, W. S.; Choi, J.-H.; Yoon, U. C.; Lee, J.-W.; Song, J.-G.; Shin, D.-M.; Gal, Y.-S. *J. Mater. Chem.* **2005**, *15*, 5029–5036.
(32) Schadt, M.; Seiberle, H.; Schuster, A. *Nature (London)* **1996**, *381*, 212–215.
(33) Schadt, M.; Seiberle, H. *J. Soc. Inf. Display* **1997**, *5*, 367–370.
(34) Obi, M.; Morino, S.; Ichimura, K. *Chem. Mater.* **1999**, *11*, 656–664.
(35) Jackson, P. O.; O'Neill, M.; Duffy, W. L.; Hindmarsh, P.; Kelly, S. M.; Owen, G. J. *Chem. Mater.* **2001**, *13*, 694–703.
(36) Kawatsuki, N.; Goto, K.; Yamamoto, T. *Liq. Cryst.* **2001**, *28*, 1171–1176.
(37) Contoret, A. E. A.; Farrar, S. R.; Jackson, P. O.; Khan, S. M.; May, L.; O'Neill, M.; Nicholls, J. E.; Kelly, S. M.; Richards, G. J. *Adv. Mater.* **2000**, *12*, 971–974.
(38) Aldred, M. P.; Contoret, A. E. A.; Farrar, S. R.; Kelly, S. M.; Mathieson, D.; O'Neill, M.; Tsoi, W. C. Vlachos, P. *Adv. Mater.* **2005**, *17*, 1368–1372.
(39) Kim, C.; Trajkovska, A.; Wallace, J. U.; Chen, S. H. *Macromolecules* **2006**, *39*, 3817–3823.
(40) Kim, C.; Wallace, J. U.; Trajkovska, A.; Ou, J. J.; Chen, S. H. *Macromolecules* **2007**, *40*, 8924–8929.
(41) Park, J.-H.; Yu, C.-J.; Kim, J.; Chung, S.-Y.; Lee, S.-D *Appl. Phys. Lett.* **2003**, *83*, 1918–1920.
(42) Ikeda, T.; Tsutsumi, O. *Science* **1995**, *268*, 1873–1875.
(43) Ikeda, T. *J. Mater. Chem.* **2003**, *13*, 2037–2057.
(44) Okano, K.; Tsutsumi, O.; Shishido, A.; Ikeda, T. *J. Am. Chem. Soc.* **2006**, *128*, 15368–15369.
(45) Merkel, P. B.; Roh, Y.; Dinnocenzo, J. P.; Robello, D. R.; Farid, S. *J. Phys. Chem. A* **2007**, *111*, 1188–1199.
(46) Wolff, T.; Görner, H. *Phys. Chem. Chem. Phys.* **2004**, *6*, 368–376.
(47) Skryshevski, Y. A.; Vakhnin, A. Y. *Mol. Cryst. Liq. Cryst.* **2005**, *427*, 207–216.
(48) Gierschner, J.; Cornil, J.; Egelhaaf, H.-J. *Adv. Mater.* **2007**, *19*, 173–191.
(49) Herkstroeter, W. G.; Lamola, A. A.; Hammond, G. *S. J. Am. Chem. Soc.* **1964**, *86*, 4537–4540.
(50) Specht, D. P.; Martic, P. A.; Farid, S. *Tetrahedron* **1982**, *38*, 1203–1211.
(51) Murov, S. L.; Carmichael, I.; Hug, G. L. *Handbook of Photochemistry*, 2nd ed.; Marcel Dekker Inc.: New York, NY, 1993.
(52) Giachino, G. G.; Kearns, D. R. *J. Chem. Phys.* **1970**, *53*, 3886–3891.
(53) Lamola, A. A.; Hammond, G. S. *J. Chem. Phys.* **1965**, *43*, 2129–2135.
(54) Hoffman, R.; Wells, P.; Morrison, H. *J. Org. Chem.* **1971**, *36*, 102–108.
(55) Ito, N.; Richert, R. *J. Chem. Phys.* **2005**, *122*, 234508/1–234508/7.
(56) Turro, N. J. *Modern Molecular Photochemistry*, University Science Books: Sausalito, CA, 1991; pp 305–..
(57) Furumi, S.; Ichimura, K. *Appl. Phys. Lett.* **2004**, *85*, 224–226.
(58) Mattes, S. L.; Farid, S. *Science* **1984**, *226*, 917–921.
(59) Kawatsuki, N.; Tachibana, T.; An, M.-X.; Kato, K. *Macromolecules* **2005**, *38*, 3903–3908.

MA702809G